A LARGE SIGNAL MODEL FOR PHONON-COOLED HOT-ELECTRON BOLOMETRIC MIXERS FOR THZ FREQUENCY APPLICATIONS

Harald F. Merkel, Erik L. Kollberg, K. Sigfrid Yngvesson

Department of Microelectronics
Chalmers University of Technology
S 412 96 Göteborg
SWEDEN

Phone: +46-31-772-1848
Fax: +46-31-164 513

Email: harald@ep.chalmers.se

Abstract

Phonon cooled hot electron bolometers (HEB) show smaller noise temperatures in mixer applications above 1THz compared to Schottky diodes or SIS devices. To determine the optimal bias point for maximum IF bandwidth and lowest noise of a HEB detailed understanding of the current-voltage characteristic is indispensable.

A complete nonlinear model for a hot electron bolometric (HEB) mixer is derived. The dynamic resistance of a superconducting film is calculated under strong demagnetization conditions. The resistance is modeled due to vortex flow and phase slip lines. Self heating gives rise to normal domains in the film. In addition the resistance due to thermally activated flux creep and thermal fluctuations is taken into account. All these relations form a large signal model for the iv-characteristics and the bias points of the device. A small signal linearization yields then conversion gain and noise temperatures. Furthermore a quality measure for HEB devices is set up by deriving the thermal coupling of the film to the substrate and the achieved critical current density from measured current-voltage characteristics.

Introduction

A hot electron bolometer (HEB) is characterized by its resistance as a function of film temperature (R(T) curve) and current-voltage (iv-)characteristics. Typically an iv curve (c.f. Figure 1 and 2) shows a very small resistance at very low voltages until a critical current is reached, increasing the device voltage further a region with very small or even negative differential resistance is encountered. Then for even higher voltages the device becomes complete normal resistive and the iv-curve exhibits then the slope of the normal resistance. Several phenomenological models have been proposed to approximate the resistive behavior of a HEB. Karasik et al. [2] proposed a broken-line model to model the device noise [11]. There the resistive transition starts with a given critical current and the resistance increases linearly until the normal resistance is reached at another experimentally determined current. With this model a different set of fitting parameters has to be applied for every substrate temperature. The sharp separation between positive and negative differential resistance regions which occurs in some devices cannot be modeled correctly. Vendik et al.[18] proposed a refinement of this model by fitting a parabola to the superconducting-resistive transition which rounds the obtained iv-curves somewhat. Recently an expansion of the temperature derivative of the R(T) curve in terms of gaussian functions has been proposed [15]. There the resistance expansion is used in a heat balance equation to calculate iv curves with self heating. This model approximates iv curves reasonably well but modeling negative resistance regions quantitatively correct requires the introduction of correction terms to the device current.

Measured current-voltage characteristics

Typical measured unpumped current-voltage characteristics for hot electron bolometers (HEB) with the film temperature as a parameter are shown below. Figure 1 shows a complete current-voltage characteristic beginning with a Meissner state area for very small voltages. Exceeding a critical current vortex flow becomes remarkable leading to the formation of phase slip lines. If one exceeds the critical voltage for hot spot formation the characteristics shows a small positive differential resistance determined by hot spot growth. Increasing the voltage further drives the device to normal state (not shown , at about 25 mV)

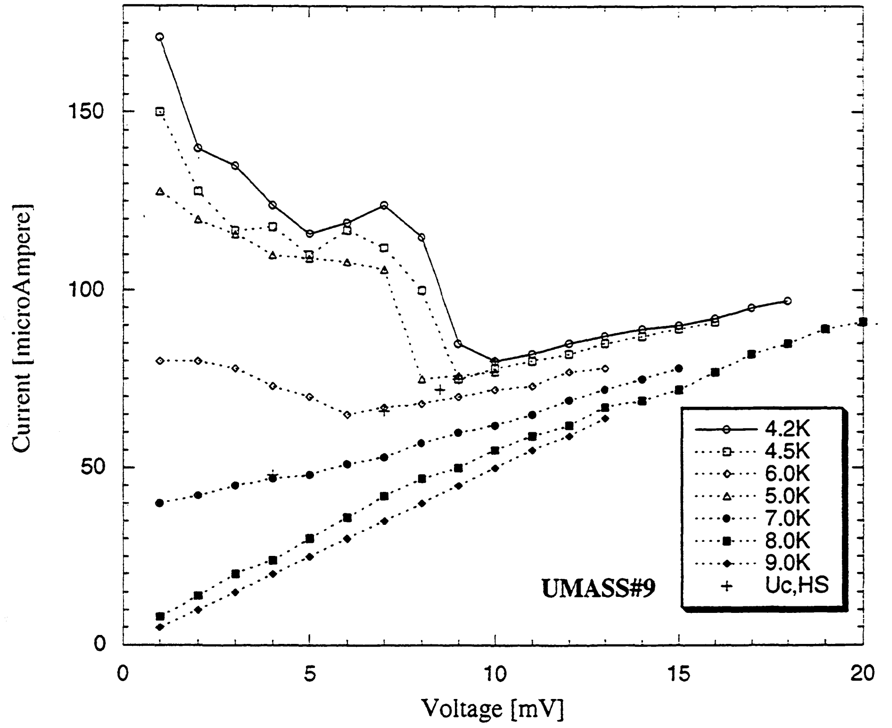

Figure 1: Unpumped current-voltage characteristic (device #9 from UMASS) for different film temperatures. The iv-curves for low temperatures (<5.0K) show a negative differential resistance behavior due to vortex flow and the formation of phase slip centers. For higher device voltages a hot spot is formed which grows until it covers the complete device. For temperatures above 9K the device becomes completely normal conducting. The crosses indicate theoretical results of the critical voltage for hot-spot formation.

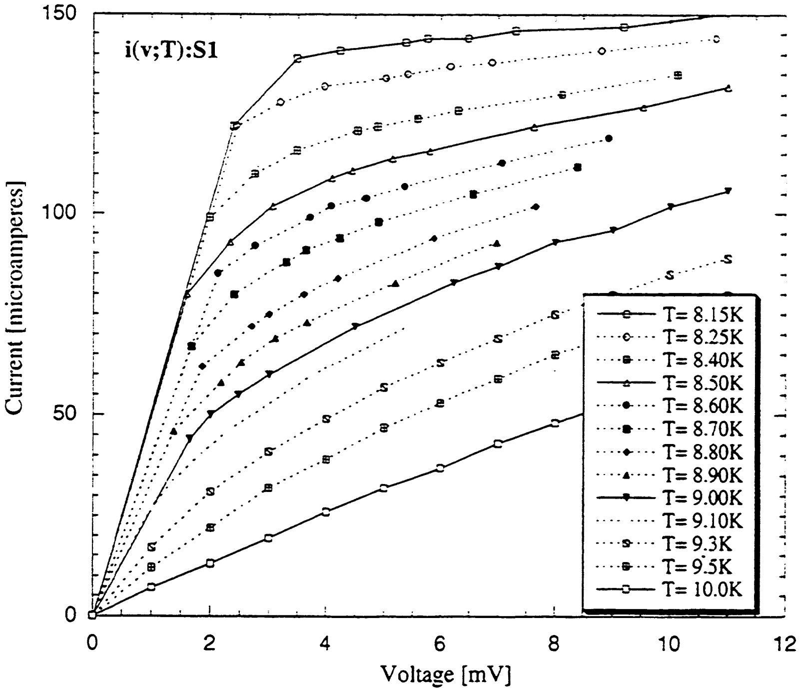

Figure 2: Unpumped current-voltage characteristic (device S1#5) for different film temperatures. The iv-curves for lower temperatures (<7.6K) show a negative differential resistance. In the bias voltage and temperature interval shown here the device is in the resistive zone as soon as the curve departs from the superconducting straight line. For temperatures above 9.9K the device becomes completely normal conducting.. The best (lowest noise and maximum bandwidth) bias points for this device is located at 8.8K/7mV. The normal resistance at 20K is about 230Ω

A typical bias point in a HEB mixer is located in the hot spot growth region. There the device is unconditionally stable (since the differential resistance is positive) but at the same time the device sensitivity to power changes is maximal. The sensitivity in the unstable region is larger than in the hot spot growth area but due to the negative differential resistance no stable operating point can be realized. Choosing the bias point close to the normal conducting state the sensitivity is very low.

In the following the device resistance will be modeled as a function of film temperature, voltage and dissipated electrical power. This requires the analysis of resistance-voltage (rv-) curves. These rv-characteristics are easily derived from the iv-characteristics in Figures 1 and 2. Figures 3 and 4 show the resistance-voltage characteristics for the devices CTH:S1 and UMASS#9. Assuming hot spot growth as the crucial resistance mechanism one has to solve a thermal power balance equation on the strip. For film temperatures in vicinity of the critical temperature this power balance can be linearized. Solving this equation the length of the hot spot is determined. The resistance of such a hot spot shows then a slope which is proportional to the difference between the film temperature and the temperature where the device becomes normal conducting. Data of device S1 exhibits this behavior: its resistance-voltage curves are almost parallel straight lines (c.f. Figure 3). Extrapolating the resistance curves to zero currents (and zero voltages) yields the resistance without any self heating. There the hot spot disintegrates and a set of vortices is left over. The vortices are still present because the resistance curves are linearly extrapolated for zero heat dissipation without changing the basic resistive effects.

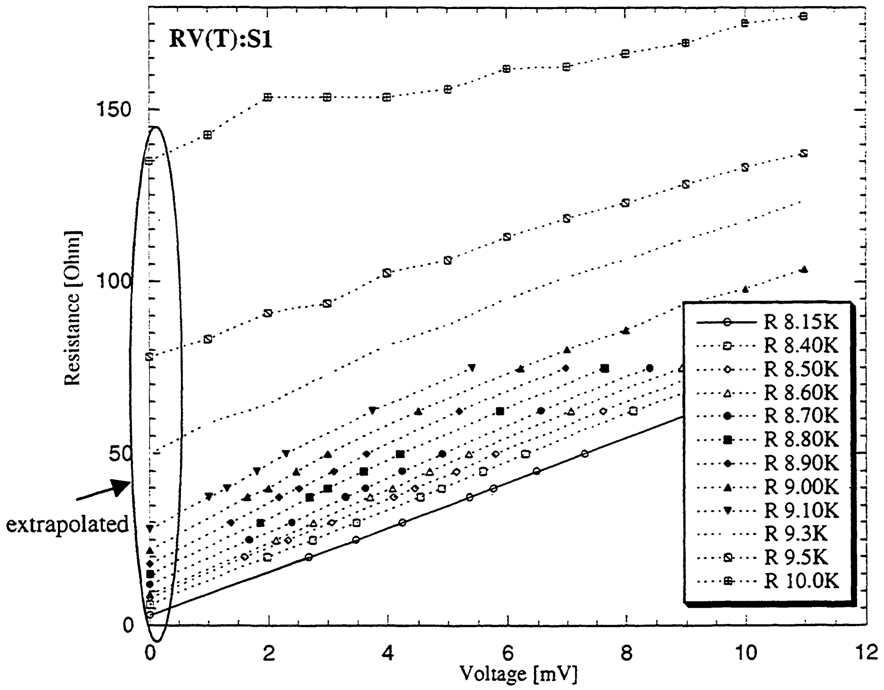

Figure 3: Unpumped resistance-voltage characteristics (device S1 , belongs to the current-voltage characteristic shown in Figure 1) for different film temperatures. The device is in hot spot growth regime. The temperature was chosen close to the critical temperature (9.9K). So no negative differential resistance region is observed. (In the measurement negative differential resistance was encountered at a film temperature of below 7.6K). The best bias points for this device is located at 8.8K/7mV

The resistance-voltage characteristics for device UMASS#9 shows a transition from the purely superconducting state (zero resistance , Meissner state) to a vortex flow / phase slip state (negative resistance region, unstable operation of the device). The resistance-voltage characteristics for the vortex state are straight lines intersecting the coordinate origin. No residual resistance is thus observed there until the film temperature is very close to the critical temperature. Then a sharp transition to normal state is observed (c.f residual resistance in Figure 5 denoted by dotted line). The instability will prevail until a hot spot is formed. Then the differential resistance becomes slightly positive.

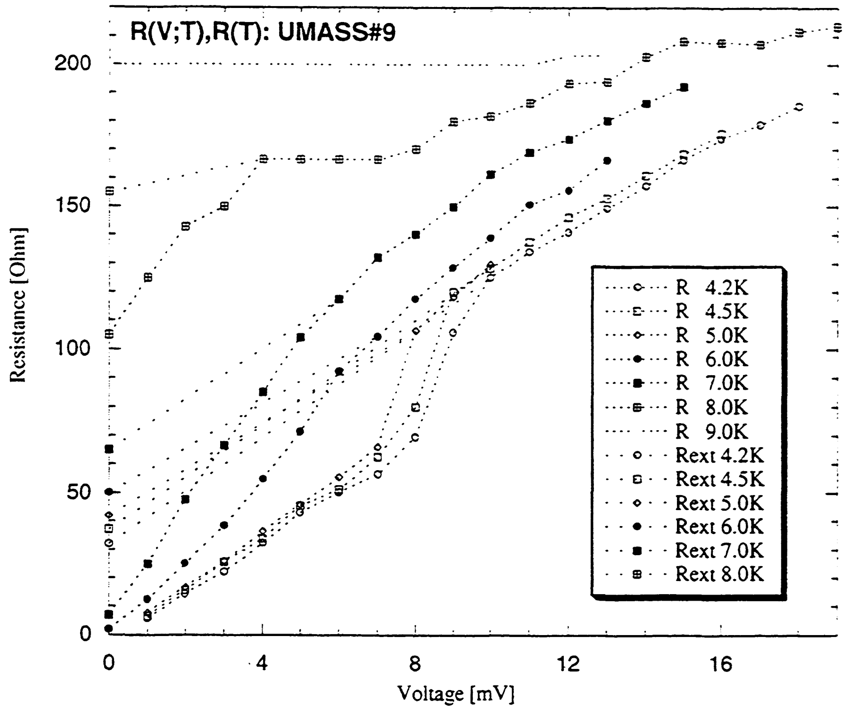

Figure 4 Device resistance as a function of device voltage for different film temperatures. The extrapolated values for the residual resistance under hot spot growth conditions (shown in Figure 5 as solid rectangles) are indicated on the y-axis. The interpolation line segments are indicated as sparse dotted lines. The interpolation of the vortex flow resistance

Device model outline

The resistance of a HEB depends on transport current, substrate temperature and heat dissipation in the superconducting film. Expanding the resistance in a power series with respect to dissipated power p and current I one obtains the following decomposition:

$$R(T,I,p)=R(T,I)\big|_{p=0}+\sum_{\mu=1}^{\infty}\frac{1}{\mu!}p^{\mu}\frac{\partial^{\mu}}{\partial p^{\mu}}R(T,I,p)\big|_{p=0}=R(T,I)\big|_{p=0}+\Delta R(T,I,p) \quad (1)$$

In Equation (1) the cold resistance (obtained for p=0) is separated in a “current free-cold” resistance and a. “dynamic resistance”.

$$R(T,I)\big|_{p=0}=R(T)\big|_{p=0,i=0}+R(I;T)\big|_{p=0} \quad (2)$$

In the subsequent text the following terms for resistances will be used:

$R(T,I)\big|_{p=0}=R_{cold}(T,I)$ This isothermal “cold” resistance excludes all self-heating effects. Thus the remaining resistive effects are due to the film temperature without any current and due to the transport current (dynamic resistance).

$R(T)\big\vert_{p=0,i=0} = R_T(T)$	denotes the current-free resistance which only depends on temperature. This resistive contribution is due to thermal fluctuations and due to thermally activated vortex flow.
$R(I;T)\big\vert_{p=0} = R_D(I;T)$	is the dynamic resistance due to transport current flow which contains the film temperature as a parameter. This resistance is caused by vortex creep / vortex flow and phase slip formation.
$\Delta R(T,I,p)$	denotes the resistance change due to self-heating. It is obtained explicitly by solving a heat balance equation on the HEB strip.

Self heating is included by solving a heat balance equation based on the "cold" resistance where the dissipated heat due to RF and bias acts as a heat source. Its solution yields an updated film temperature. Self heating results in the formation of hot spots and normal domains.

The model can be greatly simplified for the region of special interest for HEB mixer operating points: There the relevant current dependent resistive effect is hot spot growth. The "zero-current" temperature dependent resistance is determined by thermally activated flux creep.

Investigating the dynamic resistance of a superconducting strip under voltage bias the film properties will change at distinct voltages. Such a critical voltage drives a critical current at the device resistance. Assume that the device resistance jumps from a value R_{lo} to R_{hi} if the critical current is exceeded. Increasing the bias voltage to reach the critical voltage the film current will increase too and the critical current is reached. Then the resistance is increasing and which diminishes the current to a value below the critical one. Obviously a stable mixed state is reached at the voltage which drives the critical current at R_{lo}. This mixed state is stable until the voltage exceeds the voltage for which the critical current is driven even for the higher resistance R_{hi}. Above the upper critical voltage the film state becomes homogenous again.

The current-dependent resistive transition, "dynamic resistance"

As a well known fact type II superconductors allow penetration of magnetic fields in the form of localized flux quanta [5], [13], [14] if the inner magnetization exceeds the lower critical magnetic field. Demagnetization effects reduce the critical transport current needed to sustain this vortex flow. Since the mixers investigated here are operated under constant voltage conditions the critical currents have to be translated to critical voltages. Following the behavior of a superconducting film under increasing device voltage one obtains a complete Meissner state starting at very low voltages: Assuming a perfect magnetic shielding the only magnetic field present is induced by the transport current in the superconductor. The extrinsic voltage measured at the mixer pads is determined by the pad resistance only.

$$U_{c,Meissner} = R_{pad} \cdot I_{c1} = R_{pad} \cdot B_{c1} \cdot \frac{d\pi^2}{\mu_0} \cdot \left[1 - \left(\frac{T}{T_c} \right)^2 \right] \qquad (3)$$

If this extrinsic voltage is exceeded the lower critical current is reached and vortices penetrate the film. Usually if no shielding is provided the earth's magnetic field is sufficient to exceed the lower critical field so vortices will be present even then.

Phase slip line formation

Since there is always an impurity at the film surface where vortices are predominantly formed the vortices will not be equally distributed. Assume the extreme case that all vortices are generated at the same point on the film a normal conducting well will be formed perpendicular to the transport current direction if the mean distance of the vortices in this cross section becomes equal to the vortex diameter. For a phase slip line to form the vortex density (given by Equation B5 in Appendix B) the following relation must hold:

$$n_{vortex}\left(I_{c,PSL}\right) \overset{!}{=} \frac{1}{4 \cdot \xi^2} \cdot \left(\frac{\lambda_{London}}{l_{Film}} \right)^2 \qquad (4)$$

Equation (4) is used to derive a relation for the minimum current needed to sustain a phase slip. If the current exceed the phase slip critical current the film exhibits a normal conducting barrier with the resistance:

$$R_{PSL} = R_N \cdot \frac{2\xi}{l_{Film}} \tag{5}$$

A phase slip will lead to an intrinsic voltage drop which in turn reduces the transport current below the critical current leading to phase slip dissolution. The superconducting film will thus exhibit a mixed state between vortex-free regions and a weak phase-slip line which adjusts the film resistance pinning the transport current to the critical current for vortex formation. This mixed state will vanish if the (extrinsic) voltage is large enough to drive the lower critical current if the device resistance equals the phase slip line resistance:

$$U_{c,PSL} = \left(R_{pad} + R_{PSL}\right) \cdot I_{c1} = \left(R_{pad} + R_{PSL}\right) \cdot B_{c1} \cdot \frac{d\pi^2}{\mu_0} \cdot \left[1 - \left(\frac{T}{T_c}\right)^2\right] \tag{6}$$

Phase slip line resistance

According to the phase slip line (PSL) model given in [6, vol.iii , p.57] the resistance of a superconducting film carrying phase slip lines is given as:

$$R_{PSL,\infty} = R_N \cdot \frac{I_{c2}}{I} \cdot \left(\frac{I - I_{c1,film}}{I_{c2} - I_{c1,film}}\right)^2 \tag{7}$$

This relation is applicable to infinitely long films and requires the presence of more than one phase slip line whose distance depends on the device current. The films investigated here are far too short to sustain more than one phase slip line. Therefore the resistance due to phase slippage is the resistance of a single PSL.

Model for the "cold" device resistance

The device resistance is now modeled as a function of the extrinsic voltage. Thereby no self-heating effects are taken into account. The only resistance in the Meissner state is the pad resistance. The first mixed state occurs between the phase slip formation and the Meissner critical voltage. There the device resistance is at first order linearly dependent on the voltage since the transport current is pinned to the lower critical current. Exceeding the critical voltage for the phase slip line the resistance remains constant supposed that the film is short enough not to support more than one phase slip line. One obtains for the cold device resistance Equations (3,5,6,7):

$$R_{cold}(U,T,T_s) = \begin{cases} R_{pad} & U_{c,Meissner} > U \\ R_{pad} + R_{PSL} \cdot \dfrac{U - U_{c,Meissner}}{U_{c,PSL} - U_{c,Meissner}} & U_{c,PSL} > U \geq U_{c,Meissner} \\ R_{pad} + R_{PSL} & U \geq U_{c,PSL} \end{cases} \tag{8}$$

The temperature-dependent resistive transition, "zero-current resistance"

Under idealized conditions the dc-resistance of a superconductor is identically zero below the critical temperature and jumps to its normal resistance if the critical temperature is exceeded. The transition between normal and superconducting state is broadened due to thermal effects (suppressed superconductivity and diffusion of excess electrons into the strip do not play a significant role because the bridge is quite long [15]):

Below the critical temperature: Thermally activated vortex creep and thermal fluctuation

Pinned vortices present in the film will be excited thermally and will start creeping. In addition thermal fluctuations will increase the resistance below the critical temperature. Among other approximations for the current-free resistance for different temperatures [5] the best coincidence to experimental results is realized by the following relation:

$$R_T = \alpha_{flux creep} \cdot R_N \cdot e^{\frac{T-T_c}{\Delta T}} \tag{9}$$

The effective flux creep factor varies from device to device. Values for the parameters (and the hot spot length due to voltage variation needed for Equation (15)) for some devices are given in the table below .

Device	$\beta[\Omega/ \mathrm{mV}]$	$\alpha_{\mathrm{flux\ creep}}$ [1]	$R_N[\Omega]$	T_c(dipstick) [K]	ΔT [K]
CTH, S1	6.6	0.5	270	9.9	0.425
UMASS #9	6.0	1.2	185	9.0	0.43
CTH, C2 #1	6.2	1.0	150	8.5 (from iv-curve)	0.5

Table 1: Parameters for the thermally activated vortex creep resistance given by Equation (9). The data of the device UMASS#9 were measured by K.S. Yngvesson at University of Massachusetts.

To obtain the "zero current " resistance the measured data have to be extrapolated for vanishing transport currents. Measuring at currents large enough to provide vortex flow the extrapolation will yield the influence of vortex creep. If the measurement is performed at currents smaller than the lower critical current no vortex will penetrate the film and the obtained resistive transition will become very sharp.

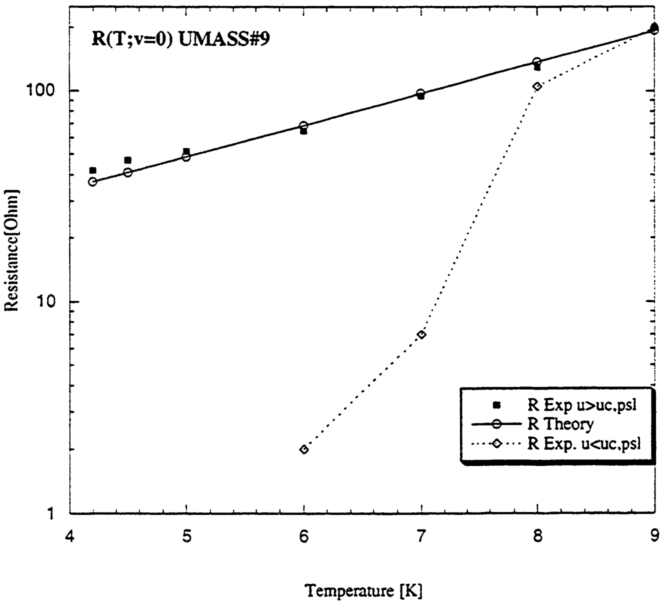

Figure 5 Logarithmic plot of the extrapolated (zero current) device resistance as a function of film temperature for the device UMASS #9. The black squares indicate extrapolated values from the hot spot growth area (c.f.Figure 3). The carets are extrapo,lated values for the vortex flow/phase slip region.

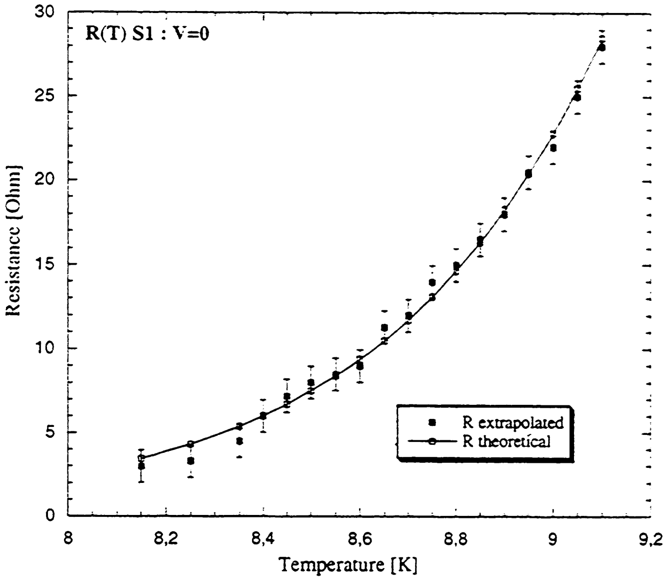

Figure 6: Device resistance as a function of temperature extrapolated for zero voltage. The theoretical curve is obtained under the assumption that thermally activated vortex flow is the only resistive process. Denote that the extrapolation to zero currents (and zero voltage) yields a "cold" resistance where self heating processes are not present. The functional relation for the theoretical curve is given by Equation [9] the needed parameters are found in the uppermost row of Table 1

Above the critical temperature: Finite lifetime of Cooper pairs, Thermal fluctuation

Above but in close vicinity of the critical temperature the measured conductivity of a superconducting thin film exceeds the normal resistance . Stochastic thermal fluctuation enable Cooper pairs to exist for a finite lifetime even above the critical temperature. These pairs will provide an additional resistance free electron transport channel and increase the macroscopically measured film conductivity. Since the HEB is typically operated in the hot-spot growth region temperatures above Tc are only reached in extended hot-spot regions. The extrapolated values of typical zero current resistances are all below the critical temperature and fit perfectly to the activated vortex creep curves.

Film self-heating

Since vortex flow and the pad resistance are quite small their contribution to device heating is negligible. Almost the whole device resistance is due to phase slip lines. Phase slip lines require the penetration of the film by vortices entering the film at a weak point. If the power dissipated in the resistor generated by the phase slip is large enough to heat the phase slip line volume to the critical temperature a stable normal domain is generated. Such a domain is called a hot spot [13]. Referring to the above steady state power balance one obtains for the minimum voltage needed to sustain a hot spot where *b* denotes the normalized thermal coupling:

$$\frac{U^2_{c,HotSpot}}{R_{PSL}} - b\cdot\left[T^{\gamma} - T^{\gamma}_{substrate}\right] = 0 \tag{10}$$

Solving Equation (10) for the voltage one is left with the minimum voltage needed to sustain a hot spot:

$$U_{c,HotSpot} = \sqrt[2]{\frac{2bR_n\xi}{l_{film}}\left(T_c^{\gamma} - T^{\gamma}_{substrate}\right)} \tag{11}$$

Theoretically obtained values of the critical hot spot voltage are depicted in Figure 1. They should coincide with the end of the negative differential resistance region of the device. Obviously the agreement with the beahvior of measured iv-curves is fairly good.

Film Temperature	**$U_{c.HotSpot}$(Tc=7.7)**	**Measured UMASS#9**
4.2K	9.503mV	9.6mV
4.5K	9.325mV	9.0mV
5.0K	8.942mV	8mV
6.0K	7.730mV	6mV (+/- 0.5mV)
7.0K	5.395mV	5mV(+/- 0.7mV)

Table 2: **Theoretical and measured critical voltages for hot-spot generation This critical voltage is determined by the upper end of the unstable region in the current-voltage characteristics. The beginning stabilization is attributed to the formation of a hot spot which exhibits a much slower time constant than phase slip lines or vortex fluids.**

Device voltages exceeding the critical voltage for hot spot formation will heat the normal domain even more and broaden it. Finally the complete film becomes normal conducting. A rough estimate for this voltage is obtained by assuming that the film temperature is uniform and equal to the critical temperature of the film. One obtains then:

$$\frac{U^2_{c,Normal}}{R_n} - b\cdot\left[T^{\gamma} - T^{\gamma}_{substrate}\right] = 0 \tag{12}$$

$$U_{c,Normal} = \sqrt[2]{\frac{bR_n}{l_{film}}\left(T_c^{\gamma} - T^{\gamma}_{substrate}\right)} \tag{13}$$

Model for the device resistance

The device resistance is now modeled as a function of the extrinsic voltage. The only resistance in the Meissner state is the pad resistance. The first mixed state occurs between the phase slip formation and the Meissner critical voltage. There the device resistance is at first order linearly dependent on the voltage since the transport current is pinned to the lower critical current. Exceeding the critical voltage for the phase slip line the resistance remains constant supposed that the film is short enough not to support more than one phase slip line. Increasing the applied voltage further the power dissipated in phase slip line is sufficient to heat the phase slip line area to the film's critical temperature. A hot spot is formed. Exceeding the critical voltage for hot spot formation the hot spot will broaden until it covers the complete film. In a last step the resistance due to thermal activation is added to the device resistance and in the calculation of the critical voltages Finally one obtains for the device resistance:

$$R(U,T)=\begin{cases} R_{pad} & U_{c,Meissner} > U \\ R_{pad} + R_{PSL}\cdot\dfrac{U-U_{c,Meissner}}{U_{c,PSL}-U_{c,Meissner}} + R_T(T) & U_{c,PSL} > U \geq U_{c,Meissner} \\ R_{pad} + R_{PSL} & U_{c,HotSpot} > U \geq U_{c,PSL} \\ R_{pad} + R_{PSL} + (R_n - R_{PSL} - R_T(T))\cdot\dfrac{U-U_{c,HotSpot}}{U_{c,Normal}-U_{c,HotSpot}} + R_T(T) & U_{c,normal} > U \geq U_{c,HotSpot} \\ R_{pad} + R_n & U \geq U_{c,normal} \end{cases} \tag{14}$$

Simplified model for typical mixer applications

Operating a HEB mixer in the hot spot growth region one typically finds resistance-voltage curves consisting of a set of almost parallel trajectories as depicted in Figure 7.
This set of parallel resistance trajectories can be explained under several assumptions:
Assume the substrate temperature to be close to the critical temperature. This allows to linearize the heat loss terms due to a temperature difference between the film and the substrate.

Secondly the differential resistance in this region is small. Since the slope of these curves is small the current is almost constant and therefore the power becomes proportional to the device voltage. Then the hot spot length becomes essentially proportional to the dissipated power.

Under this assumptions an increase in bias voltage will prolong the hot spot a certain amount which is independent of substrate temperature.
Extrapolating the resistance curves to zero currents (and zero voltages) yields the resistance without any self heating. There the hot spot disintegrates and a set of vortices is left over. The vortices are still present because the resistance curves are linearly extrapolated for zero heat dissipation without changing the basic resistive effects. The relation for the device resistance based on these assumptions becomes then :

$$R(V,T)=\alpha_{flux\,creep}\cdot R_N\cdot e^{\frac{T-T_c}{\Delta T}}+\beta\cdot V\cdot\left(T_c+\frac{1}{2}\Delta T-T\right) \tag{15}$$

The values for the parameters $\alpha_{fluxcreep}$ and β are listed in Table 1. Here $\alpha_{fluxcreep}$ denotes the efficiency to unpin a vortex in the film where β is a proportional to the (linearized) thermal coupling if the film to the substrate and describes the change of the hot spot length under voltage variations. Extrapolating this relation for zero voltage results in the residual resistance given in Equation (9) .

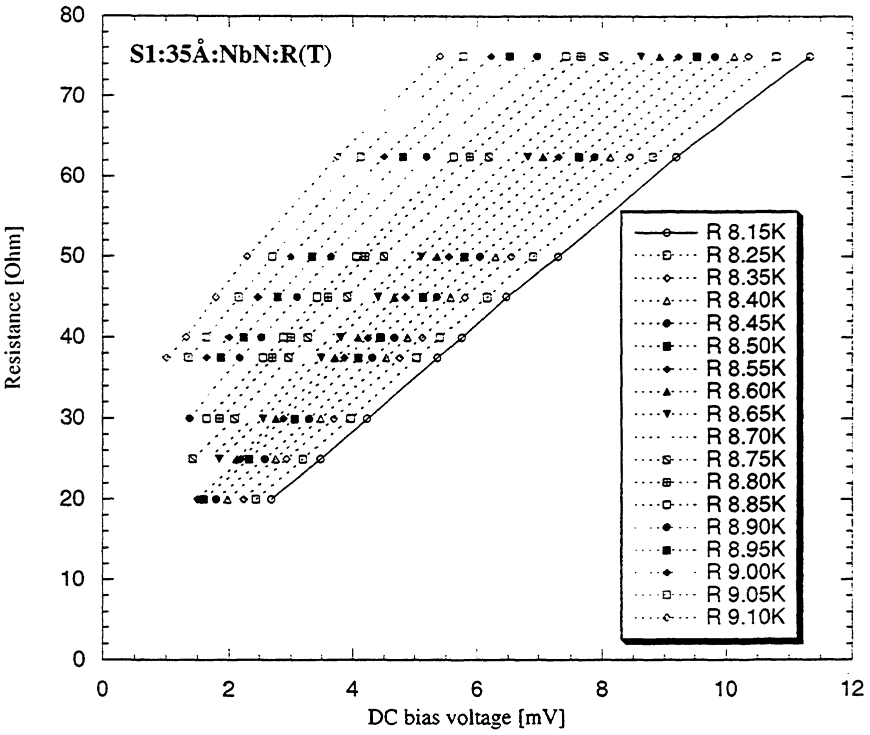

Figure 7: Unpumped resistance-voltage characteristics (device S1#4) for different film temperatures in the interval 8.15K to 9.1K. The device completely is in hot spot growth regime. This plot is a part of Figure 3 and contains the temperature interval which is most interesting for mixer operation.

Comparison to experimental data of demagnetized lower critical currents

In Figure 8 the theoretical values for a bolometer strip for a critical temperatures of 10.2K and 7.7 K are compared to measured values for a 10.2K NbN made by CTH and a 7.7K NbN (UMASS #9) HEB from University of Massachusetts.

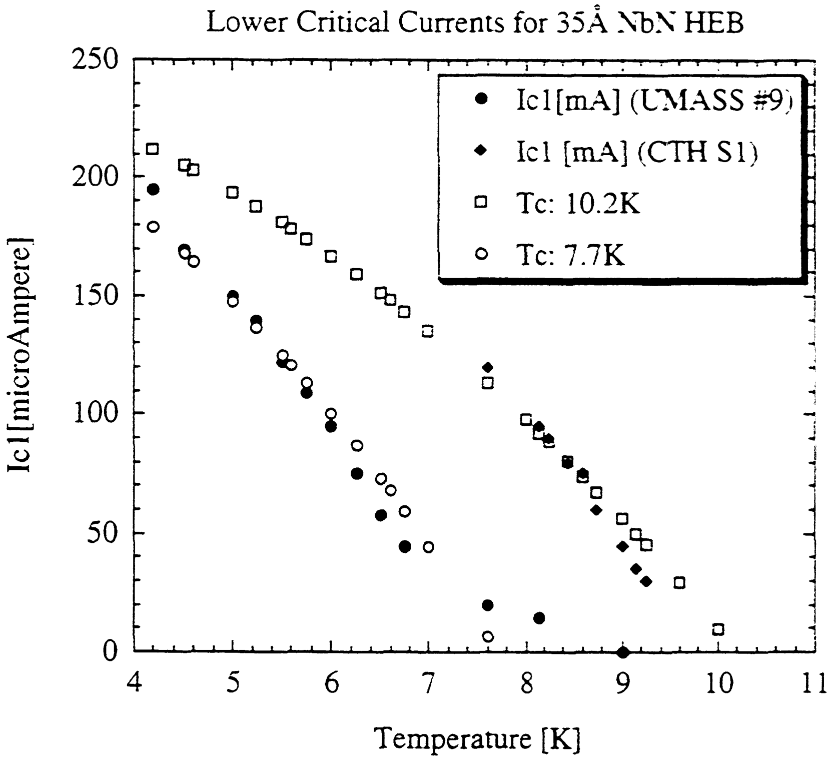

Figure 8: Critical current for the devices UMASS#9 (measured: filled circles , theoretical: empty circles) and CTH S1 (measured: filled carets , theoretical: empty squares). The data is taken from measurements of unpumped iv-characteristics for various substrate temperatures.

In the following table the theoretical ad experimentally obtained values for critical currents of a NbN bolometer strip are listed for 4.2K and 8.15 K substrate temperature. The critical current for vortex flow is considerably larger than the current for phase slip line formation which leads to the direct transition from Meissner state to phase slip lines.

Critical value	$T_{substrat}$=4.2K	$T_{substrat}$=8.15K	$T_{substrat}$=8.15K, measured
I_{c1} (Equation 3)	194.2 μA	96.0 μA	95 μA
$U_{c.Meissner}$ (Equation 3)	10.8 μV	6.2 μV	not observable
$U_{c.PSL}$ (Equation 6)	162.2 μV	91 μV	0.1mV
$U_{c.HotSpot}$ (Equation 11)	11.94 mV	4.95 mV	5 mV
$U_{c.Normal}$ (Equation 13)	168.9 mV	59 mV	>55 mV

Table 3: Theoretical critical currents and critical voltages for vortex flow, phase slip line and hot-spot formation for the device CTH:S1 for different temperatures and a comparison with data obtained from measurements.

Conclusion

In contrast to previous models for the iv-characteristic of hot-electron bolometers the resistive transition obtained directly from the physical behavior of the film and is not fitted to the experimental data. Furthermore there is a clear distinction between the "equilibrium" heating due to thermal heating and bias power which is dissipated via vortex scattering and the "nonequilibrium" heating acting on the electrons of the film only which are thermally coupled to the film phonons which in turn transfer energy to the film material. In addition the bolometer temperature is no longer assumed to be constant throughout the film. The large signal behavior of a phonon-cooled hot-electron bolometer can therefore be described using only one model parameters besides geometric and physical parameters: the thermal loss coefficient per unit square of the film to the surrounding (needed for the lateral power balance Equation (12)).Both parameters are independent of geometry and a characteristic for the film quality and the films thermal coupling to the substrate.

The knowledge of the lateral distribution of the film temperature allows the model to take the frequency behavior of the RF absorption mechanisms completely into account. The RF absorption takes place only in the film regions where the quasiparticle bandgap is smaller than the photon energy. This limits the active area where Cooper pair dissociation occurs to a frequency dependent fraction of the film explaining the curvature change of pumped iv-curves with frequency. In addition the device noise model is refined. Now vortex shot noise, Nyquist noise for the normal domains and thermal fluctuation noise are easily included because the resistance as a function of current, voltage and dissipated power is explicitly known.

Acknowledgements

The authors are deeply indebted to Dr. Pavel Yagoubov for fruitful discussions on the device physics and for the data of a complete parametric measurement for the devices CTH S1#5 and CTH C2.

Appendix A: Demagnetization and vortex flow in a type II superconducting film

Demagnetization effects

The formation of vortices is determined by the magnetic field inside the material. The magnetization at the sample surface shield a part of the applied magnetic field. The surface magnetization depends on the sample geometry. For ellipsoids (including degenerate ellipsoids like discs, rods) it can be shown [5: p.420 (applying duality theorems)] that external fields in the ellipsoids´ main axes lead to collinear demagnetization fields. Therefore the influence of surface magnetization is conveniently described by demagnetization factors in the main axes.

$$\vec{B}_{outer} \cdot \hat{x} = \vec{B}_{inner} \cdot \hat{x} - N_x \cdot \left(\vec{M} \cdot \hat{x}\right) \qquad \text{(A1)}$$

Since the surface magnetization vanishes when integrated over the whole surface, the sum of the demagnetization factors is unity. Let us consider now the case of a thin film. Applying a magnetic field normal to the film surface gives rise to a very big area which will carry depolarization currents compared to a magnetic field normal to the film edge. The demagnetization factor for a normal field is approximated by:

Defining the magnetic susceptibility of a material according to

$$\left(1+\chi\right) \cdot \mu_0 = \mu \qquad \text{(A2)}$$

one obtains for the magnetic flux density and the magnetization in a demagnetizing geometry in terms of the applied field B_{app}:

$$B_{inner} = B_{app} \cdot \frac{1+\chi}{1+\chi \cdot N} \qquad \text{(A3)}$$

$$M = B_{app} \cdot \frac{1}{\mu_0} \cdot \frac{\chi}{1+\chi \cdot N} \qquad \text{(A4)}$$

A type II superconductor in Meissner state is a perfect diamagnet with $\chi \equiv -1$ if the inner magnetic field does not exceed the first critical magnetic field

$$\mu_0 \cdot H_{inner} = \left|\mu_0 \cdot M\right| \le B_{c1} \qquad \text{(A5).}$$

In samples with non demagnetizing geometries ($N = 0$), the magnetization leads to a flux density which cancels the applied field inside the superconductor. For thin films the demagnetization factor normal to the film surface are almost unity. The magnetization in the material sample for a film with the thickness d and width w becomes then:

$$\mu_0 M = -B_{app} \cdot \frac{1}{1-N} \approx -B_{app} \cdot \frac{2}{\pi} \frac{w}{d} \qquad \text{(A6)}$$

In ultrathin and wide films the magnetization and the inner field strength reaches very big values. The applied field needed to reach the critical magnetic field in the film is reduced by $1 - N$.

$$B_{c1,demagnetized} = (1-N)B_{c1} \Rightarrow B_{c1,film} = B_{c1} \cdot \frac{\pi}{2} \frac{d}{w} << B_{c1} \qquad \text{(A7)}$$

Typical film dimensions for HEB bridges are 35Å thick and a few microns wide which leads to three orders of magnitude in reduction of the lower critical field. The upper critical field remains essentially unaffected by demagnetization effects since the susceptibility of the film in normal state is close to zero.

Lower critical transport current for vortex generation in a thin film

Based on the above equation and the relation between the total film current and its magnetic field the lower critical transport current is obtained by setting the current induced magnetic flux density equal to the lower critical flux density in a thin film assuming a square law temperature dependence of the critical fields [5:p.52]

$$I_{c1,film} \approx \pi^2 \cdot B_{c1,0K} \cdot \left(1 - \left[\frac{T}{T_c}\right]^2\right) \cdot \frac{d}{\mu_0} \qquad \text{(A8)}$$

This current is obtained by the current where the unpumped iv-characteristic departs from the pad resistance line. Sometimes the superconducting part of an unpumped iv-characteristic looks like a parabola. This is attributed to a transition resistance between the normal conducting cover layer (typical 100 nm Au film) and the superconducting bottom layer. In these cases a the lower critical current must be estimated by the point where the curve begins to deviate from the parabola. Comparison between theory and experiment obtained for 35Å NbN films are shown in Figure 8.

Appendix B: A scaling model for the susceptibility

A simple scaling model for the susceptibility of a type II superconductor is obtained as follows:

$$\chi = \begin{cases} -1 & B_{app} \le B_{c1,film} \\ -1 + \left(\dfrac{B - B_{c1,film}}{B_{c2} - B_{c1,film}}\right)^{\frac{1}{2}} & B_{c1,film} < B_{app} \le B_{c2} \\ 0 & B_{app} < B_{c2} \end{cases} \qquad \text{(B1)}$$

The susceptibility for the mixed state can be simplified by applying Ginzburg-Landau's relation between the critical fields [1:p.270] for a high-kappa approximation:

$$\frac{B - B_{c1,film}}{B_{c2} - B_{c1,film}} = \frac{2\kappa^2 \dfrac{B}{B_{c2}} - (1-N)\cdot\ln\kappa}{2\kappa^2 - (1-N)\cdot\ln\kappa} \approx \frac{B}{B_{c2}} - (1-N)\frac{\cdot\ln\kappa}{2\kappa^2} \tag{B2}$$

In a superconductor in mixed state the magnetic flux is penetrating the superconductor in flux quanta whereas the remaining material excludes the field completely. Assuming that the whole internal magnetic field is carried by flux quanta their number density is given by the difference between the magnetization obtained for the Meissner state ($\chi = -1$) and the actual mixed state ($\chi > -1$) divided by the flux quantum. For fields not exceeding the upper critical field one obtains for the number density of vortices:

$$n = \begin{cases} 0 & B_{app} \le B_{c1,film} \\ \dfrac{B_{app}}{\mu_0 \cdot \Phi_0} \cdot \left(\dfrac{\chi}{1 + \chi \cdot N} + \dfrac{1}{1-N} \right) & B_{c1,film} < B_{app} \end{cases} \tag{B3}$$

It is more convenient to express the vortex number in terms of transport current instead of lateral magnetic fields. Vortices will enter the film if there is a point where the lower critical magnetic flux is exceeded. This requires a minimum transport current through the strip which is denoted as lower critical current:

$$I_{cF1} = 2\pi w \frac{B_{c1}}{\mu_0} \approx \frac{B_{c1,bulk}}{\mu_0} \pi^2 \cdot d \cdot \left(1 - \left[\frac{T}{T_c} \right]^2 \right) \tag{B4}$$

After a lengthy but straightforward calculation one is left with the following expression for the vortex number density as a function of the transport current supposed that the current does not drive the complete film into normal state (i.e. the upper critical field is not exceeded):

$$n = \begin{cases} 0 & B_{app} \le B_{c1,film} \\ \dfrac{B_{app}}{\mu_0 \cdot \Phi_0} \cdot \left(\dfrac{\chi(B_{app})}{1 + \chi(B_{app}) \cdot N} + \dfrac{1}{1-N} \right) & B_{c1,film} < B_{app} \end{cases} \tag{B5}$$

This relation is used to determine the critical current for phase slip line formation and the resistance due to vortex flow. The vortices travel with a collision-dominated speed and give rise to a voltage drop:

$$V_{vortex\ flow} = n \cdot v_{saturation} \cdot \frac{\Phi_0}{4\pi\xi^2} \tag{B6}$$

Applying a relation between the transport current and the applied field the resistance due to vortex flow can be calculated.

References

[1] B.S. Karasik, A.I. Elantev: Analysis of the Noise Performance of a Hot Electron Superconducting Bolometer Mixer 6.th Intl. Symposium on Space Terahertz Technology Proc.: p.229

[2] H. Ekström, B.S. Karasik: Electron Temperature Fluctuation Noise in Hot Electron Superconducting Mixers Appl. Phys. Lett. 66 (23) June 1995

[3] B.S. Karasik, A.I. Elantev: Noise Temperature limit of a superconducting hot-electron bolometer mixer, Appl. Phys. Lett. 68 (6) February 1996 p.853

[4] S. Maas Nonlinear Microwave Circuits IEEE Press 1996

[5] C.P.Poole, H.C. Farach, R.J. Creswick "Superconductivity" Academic Press 1996

[6] O.Vendik,I.Vendik,High Temperature Superconductor Devices for Microwave Signal Processing . Scladen , St. Petersburg 3 volumes 1996

[7] E. Gerecht, C. F. Musante. K. S. Yngvesson, "Optical Coupling and Conversion Gain for NbN HEB Mixer at THz Frequencies" Proceedings of the 1997 Int. Semiconductor Device Research Symposium, Charlottesville, VA,, pp. 47-50, 1997.

[8] B. S. Karasik, M. C. Gaidis, W. R. McGrath, B. Bumble. H. G. LeDuc, "Low Noise in a Diffusion Cooled Hot-Electron Mixer at 2.5 THz", Appl. Phys- Lett.. vol. 71, pp. 1567-1569, 1997

[9] A. Skalare, W.R. McGrath, B. Bumble, H.G. LeDuc (1997), "Noise and RF bandwidth measurements of a 1.2THz HEB heterodyne receiver" Proc. for the 8th Int. Symp. on Space Terahertz Technology, Cambridge MA, 1998

[10] A. Skalare, W.R. McGrath, B. Bumble, H.G. LeDuc, P.J. Burke, A.A. Verheijen, and D.E. Prober (1995) A heterodyne receiver at 533 GHz using a diffusion cooled superconducting hot electron mixer,"IEEE Trans. on Applied Superconductivity, vol. 5, March 1995.

[11] H. Ekström, B. Karasik, E. Kollberg, and K.S. Yngvesson (1995) Conversion Gain and Noise of Niobium Superconducting Hot-Eelectron-Mixers, IEEE Transactions on Microwave Theory and Techniques, vol. 43, 938-947

[12] H. Merkel, E. Kollberg, "A power balance model for hot-electron bolometric mixers based on phase slip center and hot-spot formation" to appear in Proc. for the 9th Int. Symp. on Space Terahertz Technology, Pasadena, USA, 1998

[13] A. V. Gurevich and R. G. Mints (1987) Self-heating in normal metals and superconductors, Reviews of Modern Physics, vol. 59, 841-999,

[14] R. P. Huebener (1979) Magnetic flux Structures in Superconductors. Berlin: Springer.

[15]. H. Merkel, P. Yagoubov, E. Kollberg, "A Power Balance Model for Hot-Electron Bolometer Mixers at THz Frequencies, Proceedings of the 1997 Int. Semiconductor Device Research Symposium, Charlottesville, VA,, pp. 489-492, 1997.

[16]. D. Wilms Floet, J. Baselmans, J.R. Gao, and T.M. Klapwijk, Abstract for 9th Int. Symp. on Space Terahertz Technology, Pasadena, USA, 1998

[17] H. Ekstrom, E. Kollberg, P. Yagoubov, G. Gol'tsman, E. Gershenzon and S. Yngvesson, "Gain and noise bandwidth of NbN hot-electron bolometric mixers", Appl. Phys. Lett., 70(24), 1997.

[18] O. Vendik and E. Kollberg, "Conversion Loss of a Resistive State Superconductor Mixer", Proceedings of the 8th Int. Symp. on Space Terahertz Technology,, Boston, 1997.